Mol Biol Rep (2012) 39:775–784
DOI 10.1007/s11033-011-0798-y

Differential effects of *Cucumber mosaic virus* satellite RNAs in the perturbation of microRNA-regulated gene expression in tomato

Junli Feng · Leiyu Lai · Ruohong Lin · Chunzhi Jin · Jishuang Chen

Received: 26 November 2010 / Accepted: 29 April 2011 / Published online: 18 May 2011

Abstract Viral infections generally cause disease symptoms by interfering with the microRNA (miRNA)-mediated regulation of gene expression of host plants. In tomato leaves, the accumulation levels of eleven miRNAs and ten target mRNAs were enhanced by different degrees upon *Cucumber mosaic virus* (CMV)-Fny and *Tomato aspermy virus* (TAV)-Bj infections. The ability of CMV-Fny to interfere with miRNA pathway was dramatically suppressed in the addition of the benign satellite (*sat*) RNA variant (*sat*Yn12), but was slightly affected when CMV-Fny was co-inoculated with the aggressive *sat*RNA variant (*sat*T1). In plants harboring the infection of CMV-FnyΔ2b (a CMV-Fny 2b-deletion mutant), the unaltered miRNAs and target mRNAs levels compared with mock inoculated plants indicated that 2b ORF was essential for perturbation of miRNA metabolism. When the amounts of viral open reading frames (ORFs) in these infections were quantified, we found *sat*Yn12 caused a higher reduction of CMV-Fny accumulation levels than *sat*T1. These results indicate the complex mechanism by which *sat*RNAs participate in CMV-tomato interaction, and suggest that the severity of disease symptoms positively correlates to some extent with the perturbation of miRNA pathway in tomato.

Keywords *Cucumber mosaic virus* · Satellite RNA · Disease symptom · Tomato microRNA · Gene expression

Introduction

MicroRNAs (miRNAs) are an abundant subset of the plant small RNA population. They are defined by precise, dicer-like enzyme (DCL1)-catalyzed excision from the helical stems of hairpin-forming single stranded precursor RNAs [1]. Mature miRNAs are incorporated into an RNA-induced silencing complex (RISC), guide the cleavage or translational repression of endogenous target mRNAs in a sequence-specific manner. In plants, most of miRNA target genes are important transcription factors, which regulate multiple developmental processes such as organ polarity and morphogenesis, meristem identity, hormone signaling, stress responses and nutrient homeostasis [2–4].

Virus infections frequently stimulate the antiviral immune system of host plants. Similar to miRNA pathway, this is also a sequence-specific RNA degradation pathway but directed by small interfering RNAs (siRNAs), and its primary function is to restrict the accumulation and spread of exogenous virus invaders [5]. To overcome the siRNA-directed destruction of viral RNAs, most plant viruses have evolved suppressor proteins to counteract host RNA silencing [6–8]. As there are so many common features shared between the siRNA-directed RNA degradation and miRNA-mediated mRNA regulation, it is assumed the activity of viral silencing suppressors can alter miRNA metabolism through attacking common elements of the two pathways [9, 10].

Both *Cucumber mosaic virus* (CMV) and *Tomato aspermy virus* (TAV) are type species of the *Cucumovirus*, in the family *Bromoviridae* [11]. Their genomes are

Junli Feng and Leiyu Lai contributed equally to this work.

J. Feng · L. Lai · R. Lin · C. Jin · J. Chen (✉)
Institute of Bioengineering, Zhejiang Sci-Tech University, Xiasha Road #2, Hangzhou 310018, People's Republic of China
e-mail: biochenjs@163.com

J. Chen
Institute of Bioresource Engineering, Nanjing University of Technology, Nanjing, China

constituted by three single-stranded, messenger sense RNAs (RNAs 1, 2, and 3), and two subgenomic RNAs 4 and 4A, which encode five proteins designated 1a, 2a, 2b, 3a and 3b [11]. In addition, some isolates of CMV encapsidate a satellite RNA (*sat*RNA), which is a small RNA molecular that is dependent on the virus for its replication, encapsidation and spread. CMV *sat*RNAs exist as different variants, ranging from 330 to 405 nt in size, can usually attenuate or aggravate disease symptoms induced by the helper virus. CMV 2b is one of the first identified silencing suppressors [12]. Previous studies have reported the developmental abnormalities and perturbation of miRNA pathway in 2b-transgenic *Arabidopsis* are resulted from the direct interaction between 2b and Argonaut 1 (AGO1) protein, and the different effects of CMV-Fny versus CMV-Q on the miRNA pathway may be explained by differences between the two 2b proteins with respect to their stability in vivo [13, 14].

In the present work, wild type CMV-Fny, CMV-FnyΔ2b (a CMV-Fny 2b-deletion mutant), CMV-Fny-*sat*Yn12 (CMV-Fny plus a benign *sat*RNA), CMV-Fny-*sat*T1 (CMV-Fny plus an aggressive *sat*RNA), and the naturally isolated TAV-Bj were inoculated on tomato, to investigate the role of different *sat*RNAs in perturbing miRNA pathways in the course of infections. We found CMV-Fny, CMV-Fny-*sat*T1 and TAV-Bj infections significantly altered the normal miRNA-mediated gene expression regulation of host plants. However, the ability of CMV-Fny to interfere with miRNA pathway was dramatically reduced in the addition of *sat*Yn12. In combination with the levels of CMV open reading frames (ORFs) monitored during pathogenic processes, we proposed a new model by which *sat*RNAs participate in CMV-tomato interactions, and discussed the correlation between severity of disease symptoms and the perturbation of miRNA pathway in tomato.

Materials and methods

Plants, virus inoculation, and RNA extraction

Seedlings of tomato (*Solanum lycopersicum* cv. Hezuo903) were grown in a greenhouse at 16 h day/8 h night (22–28°C). CMV-Fny, the typical strain of CMV subgroup IA, was obtained by in vitro transcription of infectious cDNA clones pFny109, pFny209 and pFny309 [15]. CMV-FnyΔ2b, a mutant of CMV-Fny in which most (nt 2419–2713 of RNA 2) of the 2b ORF was deleted, was constructed as described by Du et al. [16]. CMV-Fny-*sat*Yn12 and CMV-Fny-*sat*T1 were reconstituted by co-inoculation of the corresponding in vitro transcripts of *sat*Yn12 or *sat*T1 with CMV-Fny, respectively, [17]. TAV-Bj was isolated from chrysanthemum in Beijing, China, and confirmed by ELISA (Agdia, Elkhart, IN, USA). All of the viruses were maintained on *Nicotiana tabacum*, and transferred 10–12 days before mechanically inoculating the first true leaves of 10-day old tomato seedlings. Mock-treated plants were inoculated with sodium phosphate buffer (0.1 M, pH 7.2).

At 7, 14, 21 and 28 dpi, 0.2 g tissues were sampled from the upper leaves of virus or mock inoculated plants. Total RNAs were extracted using TRIzol reagent (Invitrogen, Carlsbad, CA, USA), followed by RNase-free DNase treatment (Takara, Dalian, China).

To assess the genetic stability of these CMV variants, viral double-stranded RNAs (dsRNAs) were extracted at 35 days postinoculation (dpi), using 25 g fresh leaf tissues from CMV-FnyΔ2b infected plants, or 1–2 g tissues from other infections. Subsequently, these dsRNAs were electrophoresed by procedures described in our previous publication [17].

Primer design and real-time quantitative RT-PCR

To date, 30 tomato miRNAs have been documented in miRNA Registry database (http://miRNA.sanger.ac.uk, Release 10, Sept 2010). Among them, miR162 and miR168 are believed to participate in miRNAs biogenesis. MiR164, miR165/166, miR167 and miR319, with their respective targets mRNAs, are essential regulators of meristem initiation and maintenance, axillary meristem differentiation, and leaf morphology. MiR156, miR159 and miR171 are reported to be implicated in promoting floral transitions and regulate flowering time. Therefore, the expression alterations of these miRNAs and target mRNAs upon virus infections were determined by quantitative real-time RT-PCR (qRT-PCR) in this study.

For miRNAs quantification, their mature sequences were downloaded from miRNA Registry database, and the stem-loop RT primers, forward primers and reverse primers were designed according to criteria mentioned by Tang et al. [18]. Tomato U6 small nuclear RNA (U6snRNA) was used as the reference gene for miRNA qRT-PCR. For target mRNAs, the design of primers was based on sequences obtained from clones of *ARF8*, *AGO1-1* and *AGO1-2* in our previous work [19], or from public databases. For qRT-PCR of CMV RNAs, the gene specific primers were designed according to the sequence of each CMV-Fny ORF [15]. The 18S rRNA sequence was chosen as the reference endogenous gene for both viral RNA and mRNA relative quantification. All primer pairs were optimized and validated as per our previous work [19], and summarized in Table 1.

Table 1 List of primer sequences for real-time RT-PCR assay in this study

(a)

CMV ORF	Primer	Sequence (5′ → 3′)	Range (position)[a]
RNA1			
1a ORF	Forward	GGAGAGGAATGGGACGTGATATC	72 bp (1598–1669)
	Reverse	CAAAACTTTCCCATCGGTAACAG	
RNA2			
2a ORF	Forward	ATGAGCTCCTTGTCGCTTTTG	76 bp (361–436)
	Reverse	TTATTAAACGCAGGGCACCAT	
2b ORF	Forward	CGGCGGAAGACCATGATTT	61 bp (2681–2741)
	Reverse	CCTTCCGCCCATTCGTTAC	
RNA3			
3a ORF	Forward	CTGATCTGGGCGACAAGGA	154 bp (453–606)
	Reverse	CGATAACGACAGCAAAACAC	
3b ORF	Forward	CGTTGCCGCTATCTCTGCTAT	71 bp (1661–1731)
	Reverse	GGATGCTGCATACTGACAAACC	

(b)

mRNA	Primer	Sequence (5′ → 3′)	Related miRNA	Accession
MYB	Forward	TATTGAGATGCGGAAAGAGTTGC	miR159	AY131230 AY131231
	Reverse	ATCTGTTCGTCCTGGTAATCTTGC		
DCL1	Forward	ACTGTATCGATGTGTGCACGAG	miR162	BI209312
	Reverse	GAGTTCCAATAGAAGAGCTGCTG		
NAC1	Forward	CACCAGGATTTAGATTCCATCCA	miR164	BG791220
	Reverse	TCCTTCCCTCCAACACATGC		
HD-ZIP	Forward	CTGATTAGGGAGTCTCCTATTCTCTC	miR165/166	X91212
	Reverse	GACACTTGCTTCTGTAATCGGTC		
ARF8	Forward	TGGGAAAGGAAGAGGCTGAA	miR167	FJ222762
	Reverse	GCGATCCAAGAGATGGCATT		
AGO1-1	Forward	TGGATCAGTAACAAGCGGAGC	miR168	FJ222763
	Reverse	TTGAGAGCAGGAAGAGGTCTAACAG		
AGO1-2	Forward	ATGGAACCAGAGACATCTGACGG	miR168	FJ222764
	Reverse	CCTTACAGCAGCACCAACACC		
SCL	Forward	GATGGAGCTATGTTGTTGGGATG	miR171	DQ087265
	Reverse	CCACCAGGCTGTCCTTTCG		
TCP3	Forward	GCCTCCATGGAAACCAACTACCACT	miR319	EF091574
	Reverse	GAGCTAGCGCTATTGTTCTGCCCTA		
TCP4	Forward	AGCAAGTGCAGGGTCAAGC	miR319	EF091571
	Reverse	CTGGTGGCGAATTGAACAAG		
18S rRNA (reference gene)	Forward	GAGTCATCAGCTCGCGTTGAC		FJ710153
	Reverse	CGGATCATTCAATCGGTAGGA		

(c)

miRNA	Primer	Sequence (5′ → 3′)
miR156	RT	CTATACCATAAGCGAGGCGATCAGCAATGGTATAGGTGCTCTC
	Forward	GCCGCGTTGACAGAAGATAG
	Reverse	CATAAGCGAGGCGATCAGC
miR159	RT	GCGTGGTCCCGACCACCACAGCCGCCACGACCACGCTAGAGC
	Forward	CGTGCGTTTGGATTGAAGG
	Reverse	TCCCGACCACCACAGCC

Table 1 continued

(c)

miRNA	Primer	Sequence (5′ → 3′)
miR160	RT	CCGCGGAGCACGGAGTTGATCGAGATAGTCCGCGGTGGCATAC
	Forward	GATCATTTGCCTGGCTCCCT
	Reverse	GCACGGAGTTGATCGAGATAG
miR162	RT	GCGTGGTCCGCAGCACCTCAGCCGCCACGACCACGCCTGGATGC
	Forward	CGCAGCGTCGATAAACCTCT
	Reverse	TCCGCAGCACCTCAGCC
miR164	RT	GCGTGGTCCACACCAGTTGACGGGCGACGACCACGCTGCACG
	Forward	CACGATGGAGAAGCAGGGC
	Reverse	CCACACCAGTTGACGGGC
miR165/166	RT	CTCAGCGGCTGTCGTGGACTGCGCGCTGCCGCTGAGGGGGRATG
	Forward	CTGTGTCGGACCAGGCTTC
	Reverse	GGCTGTCGTGGACTGCG
miR167	RT	GCGTGGTCCACACCACCTGAGCCGCCACGACCACGCTAGATCAT
	Forward	CGTGCGTGAAGCTGCCA
	Reverse	TCCACACCACCTGAGCCG
miR168	RT	CTCAGCGGCTGTCGTGGACTGGGTGCTGCCGCTGAGTTCCCGAC
	Forward	CGTGTGTCGCTTGGTGCA
	Reverse	GGCTGTCGTGGACTGGGTG
miR169	RT	CTATACCATAAGCGAGCAGTAGCGCGATGGTATAGCCGGCAAG
	Forward	CGCTTACAGCCAAGGATGACT
	Reverse	CATAAGCGAGCAGTAGCGC
miR171	RT	GCGTGGTCCACACCACCTGAGCCGCCACGACCACGCGATATTGG
	Forward	CGTGCGTGATTGAGCCGT
	Reverse	TCCACACCACCTGAGCCG
miR319	RT	CTTATGCATCAGCGAGCGATAGGTGGATGCATAAGGGAGCTCC
	Forward	GCGATCTTGGACTGAAGGG
	Reverse	CATCAGCGAGCGATAGGTG
U6snRNA (reference gene)	Forward	TCTAACAGTGTAGTTTGTCCCTTCG
	Reverse	TTGTGCGTGTCATCCTTGC

[a] Data are number of nucleotide positions on CMV RNAs for start and end of each amplification fragment

The reverse transcription reactions were performed using stem-loop RT primers for miRNAs, or random primer (6 mer, Takara) for host mRNAs and CMV ORFs. A 1.0 μl aliquot of DNase-treated total RNA was inoculated with 1.0 μl of a solution containing 10 μM of each primer. The mixture was heated at 80°C for 5 min to denature the RNA, and then incubated at 60°C for 5 min to anneal the primers. After cooling to room temperature, the remaining reagents (5×buffer, dNTPs, RNase inhibitor, and M-MLV) were added according to the experimental protocol and the pulsed RT reaction proceeded for 30 min at 16°C, followed by 60 cycles at 20°C for 30 s, 42°C for 30 s, and 50°C for 1 s [18]. Finally, the reactions were heated at 85°C for 5 min to inactivate the reverse transcriptase.

PCR volumes were set up to 10 μl that contained 5 μl 2× SYBR Green PCR master mix (Takara), 1 μl of a 1:10 dilution of the cDNA template, and 800 nM each of the corresponding forward and reverse primers (as summarized in Table 1). The cycling profile was 95°C for 10 s, followed by 40 or 50 cycles of 10 s at 95°C and 30 s at 60°C. All reactions were performed in triplicate, and the controls with no template or no reverse transcription were included for each gene. Immediately after the final PCR cycle, a melting curve analysis was done to determine the specificity of each reaction. The threshold cycle (C_T) values were determined automatically by Applied Biosystem's 7300 Sequence Detection System, and the fold changes of each gene were calculated as relative quantity (RQ) values

using the comparative C_T ($2^{-\Delta\Delta Ct}$) method as per our previous work [19].

Results

Symptom expression and viral RNA accumulation in tomato infected with CMV/*sat*RNA combinations

In tomato seedlings, the disease symptoms were monitored between 7 and 35 dpi. As shown in Fig. 1, CMV-Fny infection severely altered leaf morphogenesis, inducing the typical reduction of leaflet blades and of whole-plant growth. CMV-Fny-*sat*Yn12 led to an asymptomatic infection, with plants growing with vigor and leaf size comparable to healthy controls. In contrast, the symptoms were exacerbated in CMV-Fny-*sat*T1 infection, which induced chlorosis and even necrosis of older tomato leaves, with severe mosaic and leaf distortion. CMV-FnyΔ2b infected plants exhibited slight mottle at early stages of infection but then led to general growth promotion, with increased plant height, leaf area, root length and number of lateral root than mock inoculated plants. TAV-Bj induced severe leaf mosaic, stunting and obvious shortening of internodal distances. At 35 dpi, the genetic stability of these CMV variants was confirmed by results of agarose gel electrophoresis (Fig. 2).

During the pathogenic processes, the accumulation of viral RNAs in infected tomato leaves was monitored at 7, 14, 21 and 28 dpi. As the results shown in Fig. 3, the abundance of viral RNAs in CMV-Fny-*sat*T1 or CMV-Fny-*sat*Yn12 infected plants was reduced to 0.17- to 0.83-fold of those in CMV-Fny infection at 21 dpi, respectively. For each viral RNA, the average level of four detection time points in each infection was compared and summarized in Table 2, from which we found 2a and 2b ORFs were the most significantly affected in the addition of *sat*Yn12 and *sat*T1, respectively. In the case of CMV-FnyΔ2b infection, viral RNAs levels were extremely low throughout the detection time points, almost similar to mock inoculated plants (data not shown).

Accumulation levels of miRNAs are differentially altered in CMV and TAV infected tomato plants

To investigate the interference of viral infections with miRNA pathways in tomato, the expression patterns of eleven selected miRNAs were quantified at 7, 14, 21 and 28 dpi, respectively.

As shown in Fig. 4, the expression of tested miRNAs was altered with evident strain specific differences upon different infections. Compared with mock inoculated plants, miR162, miR164 and miR168 were most significantly increased in CMV-Fny, CMV-Fny-*sat*T1 and TAV-Bj infected plants at

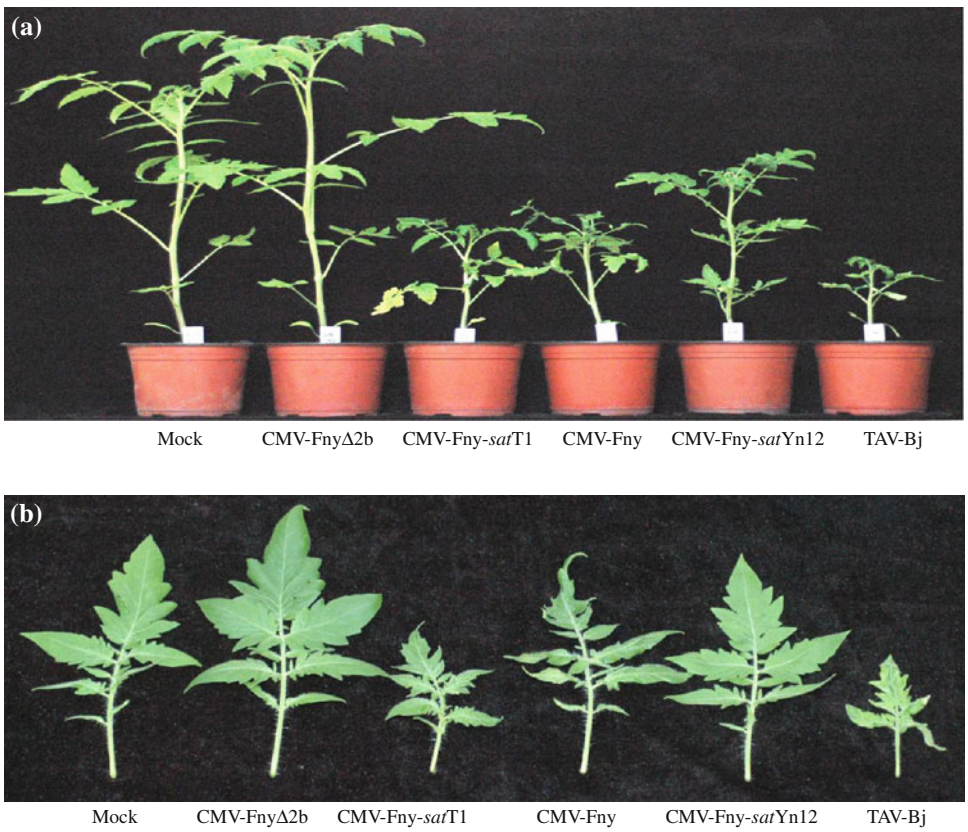

Fig. 1 Different symptoms induced by mock, CMV-FnyΔ2b, CMV-Fny-*sat*T1, CMV-Fny, CMV-Fny-*sat*Yn12 and TAV-Bj infections in tomato. At 35 days postinoculation (*dpi*), the whole plants (**a**) and the upper systemic leaves (**b**) were photographed

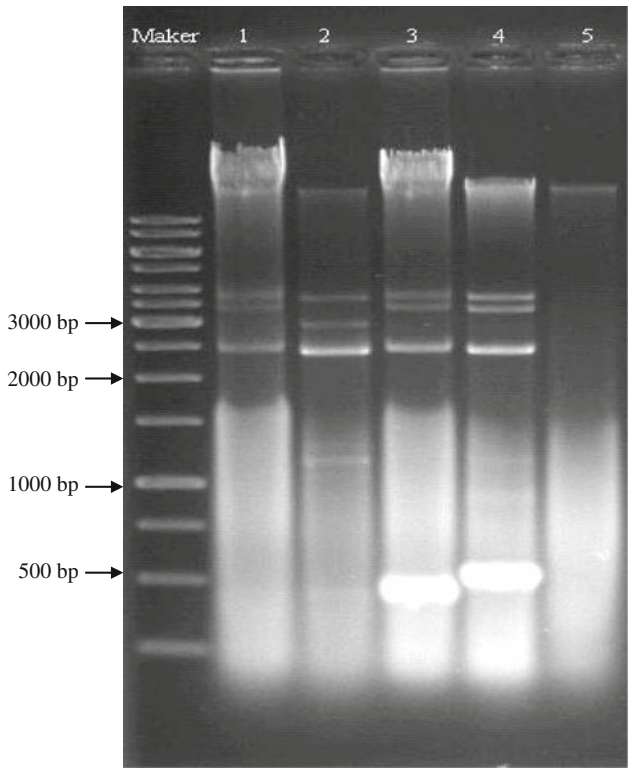

Fig. 2 Agarose gel electrophoresis of viral double-stranded RNAs (*dsRNAs*) extracted from CMV-Fny and its variants infected tomato plants at 35 days postinoculation (*dpi*). *Marker* GeneRuler^{TM} 1 kb DNA ladder (MBI fermentas); *Lane 1* CMV-Fny, *Lane 2* CMV-FnyΔ2b, *Lane 3* CMV-Fny-*sat*T1, *Lane 4* CMV-Fny-*sat*Yn12, *Lane 5* mock inoculation

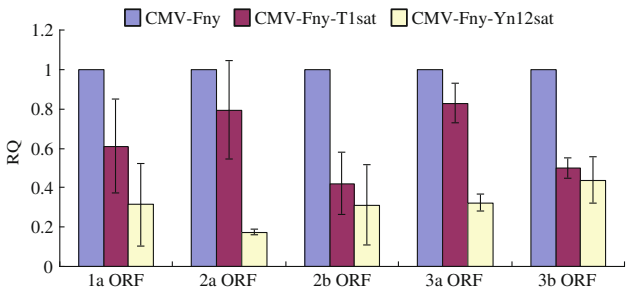

Fig. 3 The relative accumulation levels of viral open reading frames (*ORFs*) in CMV-Fny, CMV-Fny-*sat*T1 and CMV-Fny-*sat*Yn12 infected tomato leaves at 21 days postinoculation (*dpi*), determined by quantitative real-time RT-PCR. For each ORF, the expression level in CMV-Fny was set as 1, and the relative quantity (*RQ*) in CMV-Fny-*sat*T1 and CMV-Fny-*sat*Yn12 was made relative to it. 18S rRNA was chosen as an endogenous control. The results represent mean values from three biological replicates and *vertical bars* indicate standard errors

7 dpi (RQ between 5.4 and 23.1). Besides them, the abundance of miR167 was also apparently increased in these infections at 14 dpi (RQ between 4.4 and 11.2). At 21 dpi, although miR162 and miR168 remained at relatively higher levels, miR164 and miR167 in CMV-Fny-*sat*T1 infection

Table 2 Relative accumulation levels of viral ORFs in tomato leaves upon infection with CMV-Fny, CMV-Fny-*sat*Yn12 and CMV-Fny-*sat*T1

CMV ORFs	CMV-Fny	CMV-Fny-*sat*T1	CMV-Fny-*sat*Yn12
1a ORF	1.00[a]	0.78 (0.61–0.96)[b]	0.42 (0.31–0.48)[b]
2a ORF	1.00	0.60 (0.52–0.79)	0.33 (0.17–0.43)
2b ORF	1.00	0.56 (0.42–0.77)	0.37 (0.31–0.42)
3a ORF	1.00	0.76 (0.47–0.98)	0.43 (0.27–0.61)
3b ORF	1.00	0.74 (0.50–0.98)	0.48 (0.40–0.60)

[a] At 7, 14, 21 and 28 days postinoculation (*dpi*), the level of each viral ORFs in CMV-Fny infected plants was set as 1, and that in other CMV/satRNA combinations was quantified relative to it, using the $2^{-\Delta\Delta Ct}$ method

[b] For each CMV/satRNA combination, the expression level of individual viral ORF at 7, 14, 21 and 28 days postinoculation (*dpi*) was first normalized to 18S rRNA, and then made relative to the amount of corresponding ORF in CMV-Fny infection. The mean value of each ORF at four detection time points and the range of variation are shown

and miR167 in CMV-Fny infection were reduced to 4.7-, 2.1- and 5.8-fold of those in mock inoculated plants. Meanwhile, CMV-Fny and CMV-Fny-*sat*T1 induced a clear increase in miR165/166 levels (RQ > 7.0). MiR159, miR160 and miR169 were also increased in CMV-Fny or TAV-Bj infected plants to levels of approximately RQ = 5.0 at 21 dpi. At 28 dpi, the levels of miR162, miR165/166 and miR168 in CMV-Fny infection were decreased to 5.8- and 13.6-fold of those in mock, while they remained at constant levels in TAV-Bj infection. For CMV-Fny-*sat*Yn12 and CMV-FnyΔ2b infected plants, the expression levels of all tested miRNAs were not or only slightly altered throughout the time course.

Accumulation levels of miRNA-regulated genes are differentially altered in CMV and TAV infected tomato plants

Following, the transcript levels of ten miRNA-regulated mRNAs were also investigated using the same RNA preparations. Figure 5 indicated the abundance of most target mRNAs was variably enhanced after CMV-Fny, CMV-Fny-*sat*T1 and TAV-Bj infections.

In accordance with miR162 and miR168, the levels of *DCL1*, *AGO1-1* and *AGO1-2* were apparently increased in CMV-Fny infected plants at 7 dpi (RQ between 6.2 and 8.1). Other mRNAs did not show remarkable overaccumulation at this time point. At 14 dpi, CMV-Fny, CMV-Fny-*sat*T1 and TAV-Bj induced a significant increase in transcript levels of *NAC1* (RQ > 12.0), whereas *DCL1*, *AGO1-1* and *AGO1-2* in these infections were only 2.3- to 5.9-fold higher than those of in mock inoculated plants. At 21 dpi, besides *NAC1*, the levels of *MYB*, *HD-ZIP* and

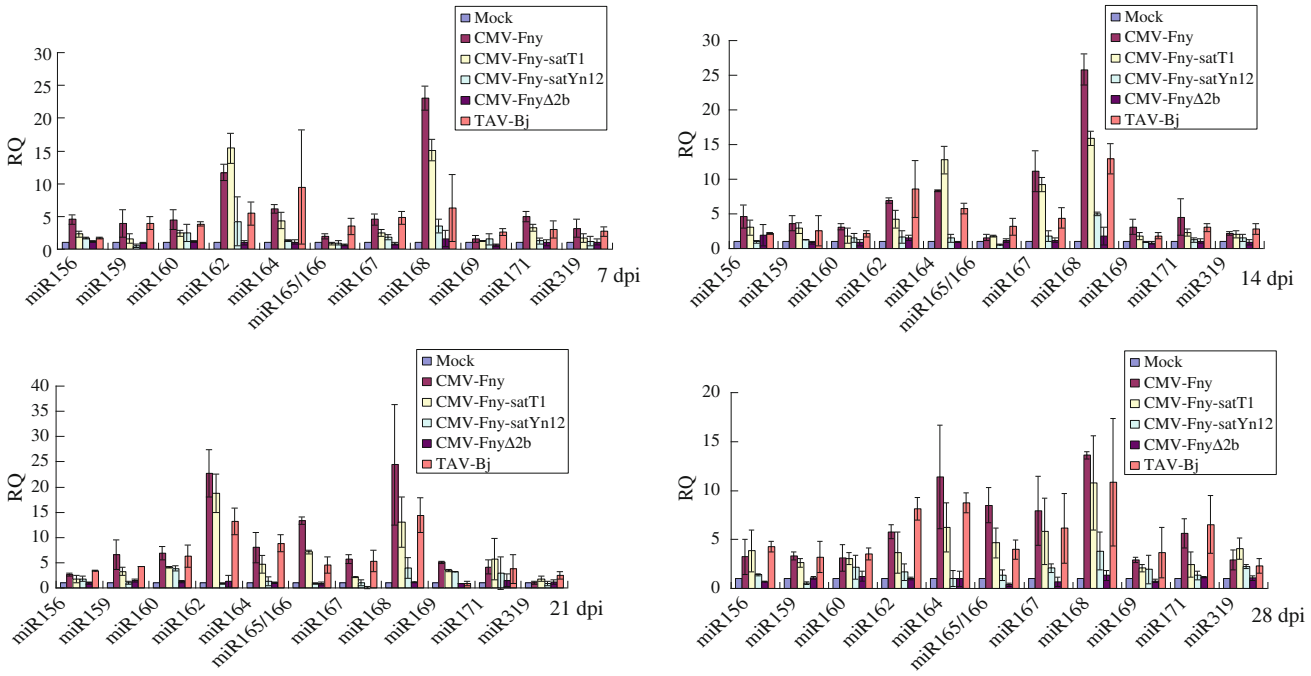

Fig. 4 Expression levels of eleven microRNAs (*miRNAs*) modulated by different virus infections in tomato plants at 7, 14, 21, 28 days postinoculation (*dpi*). According to the comparative method ($RQ = 2^{-\Delta\Delta Ct}$), the expression level of each miRNA was first normalized to 18S rRNA (reference gene), and then made relative to the amount of corresponding miRNAs in mock-inoculated sample, representing the calibrator. *Columns* represent mean fold change from three biological replicates and *vertical bars* indicate standard errors

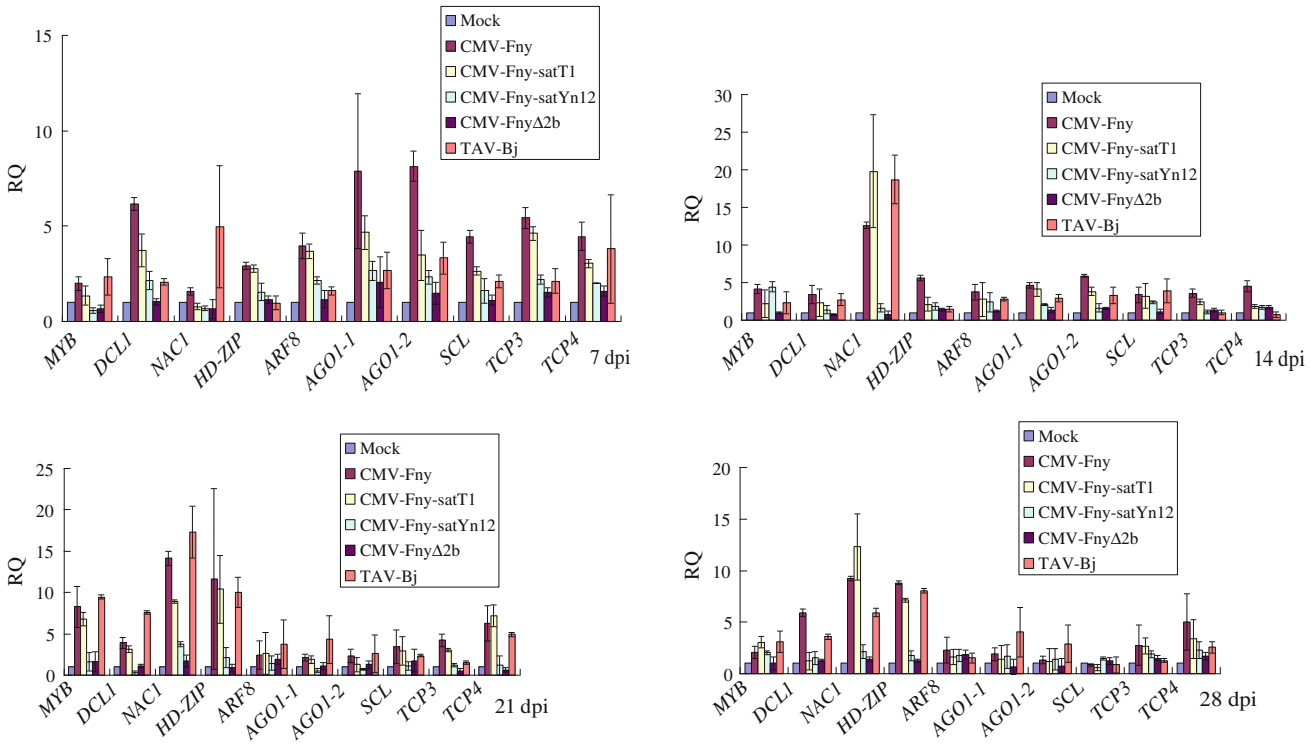

Fig. 5 Expression levels of ten target mRNAs modulated by different virus infections in tomato plants at 7, 14, 21, 28 days postinoculation (*dpi*). According to the comparative method ($RQ = 2^{-\Delta\Delta Ct}$), the expression level of each target mRNA was first normalized to 18S rRNA (reference gene), and then made relative to the amount of corresponding mRNAs in mock-inoculated sample, representing the calibrator. *Columns* represent mean fold change from three biological replicates and *vertical bars* indicate standard errors

TCP4 were also notably increased in CMV-Fny, CMV-Fny-*sat*T1 and TAV-Bj infected plants (RQ > 6.0). At 28 dpi, the abundance of *TCP4* and *MYB* was decreased to 5.0- and 2.0-fold of those in mock inoculated plants, whereas *NAC1* and *HD-ZIP* remained at relatively constant levels (approximately RQ = 9.0).

Taken together, we found besides *AGO1* and *DCL1*, the expression levels of *TCP4*, *NAC1*, *HD-ZIP* and *MYB* in CMV-Fny, CMV-Fny-*sat*T1 and TAV-Bj infected plants were also significantly altered during the pathogenic processes. When miRNAs and mRNAs were considered together, the abundance of most target mRNAs varied with the same tendency of their corresponding miRNAs, with higher values due to CMV-Fny, CMV-Fny-*sat*T1 and TAV-Bj infections, but no or very limited changes induced by CMV-Fny-*sat*Yn12 and CMV-FnyΔ2b compared with mock inoculated plants. Our data demonstrate that although with some exceptions, there is a substantial correlation between the accumulation levels of target mRNAs and the corresponding miRNA species. Moreover, these results also indicate that the addition of benign and aggressive *sat*RNAs in CMV-Fny inoculum would differentially perturb miRNA-guided regulation of gene expression.

Discussion

It is well documented that the presence of *sat*RNA results in a depression of the accumulation of CMV to a degree that varies with the isolate of CMV and the variant of *sat*RNA that interact [11, 20]. In our study, we found *sat*Yn12 caused a higher reduction of CMV-Fny accumulation levels than *sat*T1. These data completely match those of Cillo et al. [21], who reported that the benign *sat*RNA variant induced much less CMV RNAs than the aggressive *sat*RNAs in tomato. However, the substantial down-regulation of CMV 2b ORF in both *sat*Yn12 and *sat*T1 co-inoculation indicated that the attenuated disease symptoms in the addition of *sat*Yn12 could not simply attribute to the low levels of 2b gene, and consequently the reduced amounts 2b proteins, then the reduced ability to interfere with miRNA pathway, as the mechanism proposed by Cillo et al. [22] based on the study of *sat*Tfn (a mild *sat*RNA variant). It would be more appropriate to presume that the high levels of *sat*RNAs in these plants might affect the function of 2b protein through certain mechanisms, thus 2b could not effectively disrupt siRNA-directed defensive pathway of host plants, and then the replication of viral RNAs was inhibited. But obviously, more directly evidences are required to support our opinion.

In our study, the interference of viral infection with miRNA pathways in tomato was indicated by the alteration of miRNAs and target mRNA expression levels. Based on the obtained results, we found the severity of CMV disease symptoms correlated with the extent to which miRNA pathway was disrupted in the co-inoculation of *sat*Yn12. But in the addition of *sat*T1, although disease symptoms were obviously aggravated, no obvious differences were found between the miRNAs or mRNAs expression levels between CMV-Fny and CMV-Fny-*sat*T1 infections. As the chlorosis and necrosis phenotype appeared on the older leaves of CMV-Fny-*sat*T1 infected plants, whereas the samples were harvested from newly developed leaves in our study, thus further studies are needed to investigate if these results will be affected by the position of the leaves that are sampled.

CMV 2b is shown to be a multifunctional protein involved in symptoms induction, viral movement, suppression of RNA silencing, and as an antagonist of the salicylic acid-mediated defense response [16, 23]. In our study, we found the deletion of 2b coding sequence not only effectively prevented the systemic spread of this CMV-Fny mutant in tomato, disease symptoms and viral RNAs accumulation levels (data not shown) were substantially suppressed as well. Meanwhile, the expression levels of tested miRNAs and mRNAs were almost unaltered throughout the detection time points in CMV-FnyΔ2b infected plants. These data substantiate earlier studies demonstrating the role of 2b in perturbing miRNA pathway and in virulence determination again.

Although different disease symptoms were induced in tomato seedlings infected with CMV-Fny and TAV-Bj, no apparent differences were observed between the expression alterations of tested miRNAs and target mRNAs in the two infections. Thus, we can not conclude if the two viruses have a similar mechanism in perturbing miRNA pathway.

The mRNAs quantification results have shown that, three genes with the known role in tomato leaf morphogenesis, *NAC1*, *HD-ZIP* and *TCP4*, were up-regulated during the pathogenic processes after CMV-Fny, CMV-Fny-*sat*T1 and TAV-Bj infections. *NAC1* is regulated by miR164, it has been reported that *NAC1* controls lamina outgrowth on a grander scale than that of serrations [24]. Reduction of *NAC* gene function in a wide range of compound leaved plants reduces the number of leaflet and results in leaflet fusions as well as suppressing serrations [25, 26]. MiR165/166-regulated *HD-ZIP* is important for establishing the adaxial cell fate during leaf dorso-ventral patterning. MiR319-regulated *TCP4* is also indispensable for proper leaf morphogenesis and leaf senescence [24, 27]. These data are in agreement with the observed leaf-altered morphology caused by CMV-Fny, CMV-Fny-*sat*T1 and TAV-Bj infections.

In our study, the miR164 and *NAC1* levels were noticeably increased in leaves of CMV-Fny, CMV-Fny-*sat*T1 and TAV-Bj infected tomato. The up-regulation of miR164/*NAC1* levels were also observed in root and leaf tissues of CMV-Fny 2b transgenic *Arabidopsis* plants [13].

As miR164/*NAC1* are believed to involve in phytohormone response pathways, this probably occurred because tomato auxin signaling pathway was perturbed by virus infections, resulting in modulated root and leave phenotypes. In a very recent article, Lewsey et al. [28] reported the disruption of *Arabidopsis* salicylic acid (SA) and jasmonic acid (JA)-mediated defensive signaling pathways by CMV 2b protein, which was consistent with our speculation. However, they suggested the 2b protein may not be the only CMV-encoded factor that inhibits JA responses in *Arabidopsis* [28]. But according to our results and the reports of Cillo et al. [22], the effects of other viral factors on miRNAs or mRNAs expression were not apparent, which probably due to the limited transcripts studied.

We found the accumulation levels of *ARF8* and *SCL* were not significantly altered in any of the five infections in tomato leaves. These results are consistent with their functions, as *ARF8* is reported to regulate the development of lateral root through auxin signaling pathway, and *SCL* is regarded to control the development of floral tissues [2, 29]. However, the abundance of *MYB*, which is believed to regulate flowering time and anther development, was significantly increased in CMV-Fny, CMV-Fny-*sat*T1 and TAV-Bj infected leaves at 21 dpi. As the mechanism of up-regulation appears to be non-miRNA mediated, we suspect these may result from spatio-temporal variation in transcription of individual mRNA [30, 31].

In conclusion, this study monitored the accumulation of viral ORFs, and quantified the expression changes of several miRNAs and their target mRNAs during the pathogenic processes, upon different CMV variants and TAV-Bj infections. Based on our observation, we find the miRNA pathway is implicated in the modification of disease symptoms in the presence of CMV *sat*RNAs. It is expected this studies will broaden our understanding of the relationship between CMV infection, *sat*RNA effects, miRNA pathway and symptom modifications in plants.

Acknowledgments This work was supported by the grants from the National Natural Science Foundation of China (30800716) and the Science Foundation of Zhejiang Sci-Tech University (ZSTU) under Grant No. 1016816-Y.

References

1. Voinnet O (2009) Origin, biogenesis, and activity of plant microRNAs. Cell 136:669–687
2. Chuck G, Candela H, Hake S (2009) Big impacts by small RNAs in plant development. Curr Opin Plant Biol 12:81–86
3. Lu XY, Huang XL (2008) Plant miRNAs and abiotic stress responses. Biochem Biophys Res Co 368:458–462
4. Schwab R, Palatnik JF, Riester M, Schommer C, Schmid M, Weigel D (2005) Specific effects of microRNAs on plant transcription. Dev Cell 8:517–527
5. Mlotshwa S, Pruss GJ, Vance V (2008) Small RNAs in viral infection and host defense. Trends Plant Sci 13(7):375–382
6. Chapman EJ, Prokhnevsky AI, Gopinath K, Dolja VV, Carrington JC (2004) Viral RNA silencing suppressors inhibit the microRNA pathway at an intermediate step. Genes Dev 18:1179–1186
7. Dunoyer P, Lecellier C, Parizotto EA, Himber C, Voinnet O (2004) Probing the microRNAs and small interfering RNA pathways with virus-encoded suppressors of RNA silencing. Plant Cell 16:1235–1250
8. Levy A, Dafny-Yelin M, Tzfira T (2008) Attacking the defenders: plant viruses fight back. Trends Microbiol 16(5):194–197
9. Bazzini AA, Hopp HE, Beachy RN, Asurmendi S (2007) Infection and coaccumulation of tobacco mosaic virus proteins alter microRNA levels, correlating with symptom and plant development. Proc Natl Acad Sci USA 104:12157–12162
10. Berkhout B, Haasnoot J (2006) The interplay between virus infection and the cellular RNA interference machinery. FEBS Lett 580:2896–2902
11. Palukaitis P, Garcia-Arenalt F (2003) Cucumoviruses. Adv Virus Res 62:241–323
12. Ruiz-Ferrer V, Voinnet O (2007) Viral suppression of RNA silencing: 2b wins the Golden Fleece by defeating Argonaute. BioEssays 29:319–323
13. Lewsey M, Robertson FC, Canto T, Palukaitis P, Carr JP (2007) Selective targeting of miRNA-regulated plant development by a viral counter-silencing protein. Plant J 50:240–252
14. Zhang X, Yuan YR, Pei Y, Lin SS, Tuschl T, Patel DJ, Chuan NH (2006) *Cucumber mosaic virus*-encoded 2b suppressor inhibits Arabidopsis Argonaute 1 cleavage activity to counter plant defense. Genes Dev 20:3255–3268
15. Feng JL, Chen SN, Tang XS, Ding XF, Du ZY, Chen JS (2006) Quantitative determination of *cucumber mosaic virus* genome RNAs in virions by real-time reverse transcription polymerase chain reaction. Acta Biochem Biophys Sin 38(10):669–676
16. Du ZY, Chen FF, Zhao ZJ, Liao QS, Palukaitis P, Chen JS (2008) The 2b protein and C-terminus of the 2a protein of *Cucumber mosaic virus* subgroup I strains both play a role in viral RNA accumulation and induction of symptoms. Virology 380:363–370
17. Liao QS, Zhu LP, Du ZY, Zeng R, Chen JS (2007) Satellite RNA-mediated reduction of *cucumber mosaic virus* genomic RNAs accumulation in *Nicotiana tabacum*. Acta Biochem Biophys Sin 39(3):217–223
18. Tang F, Hajkova P, Barton SC, Lao K, Surani MA (2006) MicroRNA expression profiling of single whole embryonic stem cells. Nucleic Acids Res 34:e9
19. Feng JL, Wang K, Liu X, Chen SN, Chen JS (2009) The quantification of tomato microRNAs response to viral infection by stem-loop real-time RT-PCR. Gene 437:14–21
20. Escriu F, Fraile A, Garcia-Arenal F (2000) Evolution of virulence in nature populations of the satellite RNA of *cucumber mosaic virus*. Phytopathology 90:480–485
21. Cillo F, Pasciuto MM, De Giovanni C, Finetti-Sialer MM, Ricciardi L, Gallitelli D (2007) Response of tomato and its wild relatives in the genus Solanum to *cucumber mosaic virus* and satellite RNA combinations. J Gen Virol 88:3166–3176
22. Cillo F, Mascia T, Pasciuto MM, Gallitelli D (2009) Differential effects of mild and severe *cucumber mosaic virus* strains in the perturbation of microRNA-regulated gene expression in tomato map to the 3′ sequence of RNA 2. Mol Plant-Microbe Interact 22:1239–1249
23. Ji LH, Ding SW (2001) The suppressor of transgene RNA silencing encoded by *cucumber mosaic virus* interferes with salicylic acid-mediated virus resistance. Mol Plant-Microbe Interact 14:715–724
24. Kinder CA (2010) The many roles of small RNAs in leaf development. J Genet Genomics 37:13–21

25. Berger Y, Harpaz-Saad S, Brand A, Melnik H, Sirding N, Alvarez JP, Zinder M, Samach A, Eshed Y, Ori N (2009) The NAC-domain transcription factor GOBLET species leaflet boundaries in compound tomato leaves. Development 136:823–832
26. Blein T, Pulido A, Vialette-Guiraud A, Nikovics K, Morin H, Hay A, Johansen IE, Tsiantis M, Laufs P (2008) A conserved molecular framework for compound leaf development. Science 322:1835–1839
27. Garcia D (2008) A miracle in plant development: Role of microRNAs in cell differentiation and patterning. Semin Cell Dev Biol 19:586–595
28. Lewsey MG, Murphy AM, MacLean D, Dalchau N, Westwood JH, Macaulay K, Bennet MH, Moulin M, Hanke DE, Powell G, Smith AG, Carr JP (2010) Disruption of two defensive signaling pathways by a viral RNA silencing suppressor. Mol Plant-Microbe Interact 7:835–845
29. Yang T, Xue L, An L (2007) Functional diversity of miRNA in plant. Plant Sci 172:423–432
30. Kasschau KD, Xie Z, Allen E, Llave C, Chapman EJ, Krizan KA, Carrington JC (2003) P1/Hc-Pro, a viral suppressor of RNA silencing, interferes with *Arabidopsis* development and miRNA function. Dev Cell 4:205–217
31. Valoczi A, Varallyay E, Kauppinen S, Burgyan J, Havelda Z (2006) Spatio-temporal accumulation of microRNAs is highly coordinated in developing plant tissues. Plant J 47:140–151